0.7 anomaly due to the Rashba interaction in a nonuniform electric field

J. H. Hsiao,[1] K. M. Liu,[2] S. Y. Hsu,[2] and T. M. Hong[1]
[1]*Department of Physics, National Tsing Hua University, Hsinchu 30043, Taiwan, Republic of China*
[2]*Department of Electro-physics, National Chiao Tung University, Hsinchu 30010, Taiwan, Republic of China*
(Received 22 September 2008; published 15 January 2009)

We demonstrate that three conductance features, 0.5 and $0.7G_0$ plateaus and a dip at $0.5G_0$, observed in quantum point contacts (QPCs) can be consistently explained by the Rashba interaction in the nonuniform electric field created by the side gates along the transport direction. A quantity γ is defined which depends on the extent of this nonuniformity and the electron density. A short QPC tends to have a small γ. Only when γ is large will the Rashba interaction produce a potential well deep enough to localize the electron. This provides the bound state that forms the Kondo resonance with the tunneling electrons. We propose to compare the medium/long QPC to small/large quantum dots, which are governed by the Kondo physics and the Coulomb blockade, respectively. The relation between 0.7 anomaly and the side-gate voltage, length of QPC, and temperature can all be determined to agree qualitatively with the experiments.

DOI: 10.1103/PhysRevB.79.033304 PACS number(s): 73.21.Hb, 73.63.Nm, 31.15.aj, 72.10.Fk

The puzzle of 0.7 anomaly in the quantum point contacts (QPCs) has attracted much attention,[1] but there is no consensus on its physical origin yet. One model,[2,3] taking the hint from the zero-bias anomaly (ZBA) observed experimentally, linked it to the Kondo model with the necessary local moment coming out of the spin-density-functional theory[2] (SDFT). Another competing model proposed by Pepper and co-workers[4,5] ascribed it to the spontaneous spin polarization because the $0.7G_0$ plateau was observed to evolve smoothly to $0.5G_0$ as the magnetic field is applied. The reason why they did not believe the Kondo model was perhaps that[6] the assumption and calculations involved in SDFT were not intuitive, not to mention the alternative assumption of planting a magnetic impurity within a QPC. In this work, we propose a more direct mechanism via the Rashba coupling to generate the necessary moment for the Kondo model, which is being carried by the intrinsic rather than the impurity electron trapped in the naturally formed potential well within a QPC. However, this requires a dilute electron density or a highly nonuniform electric field[7] from the side gates, which shall be measured by a quantity γ. Roughly, a short QPC tends to have a small γ. Only when γ is large will the well be deep enough to localize the electron and provide the magnetic moment that forms the Kondo resonance with tunneling electrons. We propose to compare the medium/long QPC to small/large quantum dots[8] (QDs), which are governed by the Kondo physics and the Coulomb blockade (CB), respectively. Once this contrast is established, the conductance can be calculated[2] by including the Coulomb interaction, exchange energy, and other many-body effects.

There is an intrinsic uniform electric field $\vec{E}$ in the z direction perpendicular to the two-dimensional electron-gas (2DEG) plane in the GaAs/AlGaAs heterostructures. We can apply a top gate to manipulate E_z and control the strength of the Rashba interaction (RI) which is proportional[9,10] to E_z. In a QPC device, E_z within the side gates will be larger than the top gates because the geometry of the former attracts more charges. We shall first demonstrate that the nonuniform E_z within a QPC will form an effective potential well due to the Rashba interaction $\alpha\vec{\sigma}\cdot\vec{P}\times\vec{E}(x)$, where $\vec{\sigma}$ represents a vector of the Pauli matrices and $\vec{P}$ is the momentum operator. The Hamiltonian consists of

$$H = \frac{P_x^2}{2m_{\text{eff}}} - \alpha\frac{\sigma_y}{2}[P_x, E_z(x)] + \frac{P_y^2}{2m_{\text{eff}}} + V + \alpha\sigma_x P_y E_z(x), \tag{1}$$

where m_{eff} is the effective mass of the charge carriers.

In Eq. (1), we assume that $V(x,y)=m_{\text{eff}}\varpi_y^2(x)y^2/2$ is the potential of the QPC confinement[2] where $\varpi_y(x) \sim eV_g/\hbar\cosh^2(\kappa x)$ and $\kappa\sim 1/L$ with V_g denoting the side-gate voltage and L denoting the length of the QPC. The RI with an x-dependent $E_z(x)$ can be controlled by V_g. We denote the first two terms in Eq. (1) by H_x and the remaining by H_y. Appealing to the separation of variables, the eigenfunction can be expressed as $\phi(x,y)=\Sigma_n\varphi_n(x)\chi_{nx}(y)$ with components satisfying

$$(H_x + \varepsilon_{nx})\varphi_n(x) = \Xi\varphi_n(x), \tag{2}$$

$$H_y\chi_{nx}(y) = \varepsilon_{nx}\chi_{nx}(y). \tag{3}$$

The y component in Eq. (3) is calculated to give

$$\varepsilon_{nx} = \left(n + \frac{1}{2}\right)\hbar\varpi_y(x) - \frac{m_{\text{eff}}}{2}[\alpha E_z(x)\sigma_x]^2, \tag{4}$$

where $n=0,1,2,\ldots$ are channels due to the confinement in the y direction which result in the integer-G_0 plateaus of the QPC.[11] Substituting Eq. (4) into Eq. (2) gives

$$H_x^{\text{eff}} = \frac{P_x^2}{2m_{\text{eff}}} - \alpha\frac{\sigma_y}{2}[2E_z(x)P_x - \imath\hbar\partial_x E_z(x)] + \varepsilon_{nx}. \tag{5}$$

The relative magnitude of the two terms in the square brackets of Eq. (5) is equivalent to computing $\lambda_F\partial_x E_z(x)/E_z(x)$, the product of Fermi wavelength λ_F, and the variation in E_z relative to its strength. We denote the maximum value of this quantity within the QPC by γ. The λ_F is controlled by the top gates, while the nonuniformity of E_z is determined by the length of QPC. The $\gamma\ll 1$ corresponds to the case of short QPC and small λ_F because E_z is

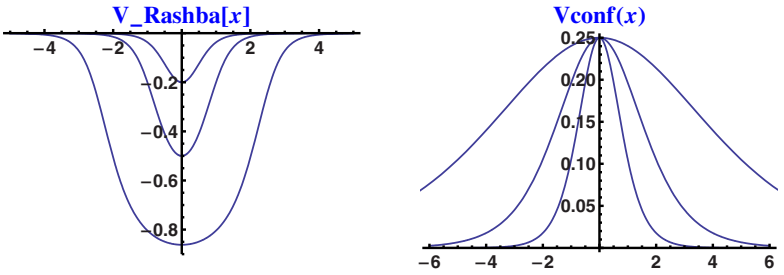

FIG. 1. (Color online) The three curves in both panels represent $L=1$, 2, and 5 ($\times 100$ nm), respectively, from the innermost. The V_{conf} in the left panel is higher in the middle of the QPC due to the y-direction confinement. In contrast, V_{Rashba} in the right panel is lower due to a stronger E_z. These two terms compete, and the formation of a sharp potential well to sustain bound states occurs when $\gamma \gg 1$.

uniform along the channel $E_z(x) \sim E_z^0$. This leads to $H_x^{\text{eff}} \simeq P_x^2/2m_{\text{eff}} - \alpha\sigma_y E_z^0 P_x + \varepsilon_{nx}$ which exhibits the normal Rashba effect which shifts the dispersion of up and down spins uniformly along the x direction with $\lambda_F^{\downarrow} < \lambda_F^{\uparrow}$. On the other hand, $\gamma \gg 1$ suits medium/long QPC with large V_g or large λ_F for which E_z is nonuniform. In this case, the $\imath\hbar\partial_x E_z(x)$ term is crucial to form a sharp potential well and trap electrons in a narrow/broad region. The electron trapped in the narrow region provides the local magnetic moment for the Kondo effect; in contrast the broad region causes the CB phenomenon.[8] An interesting scenario occurs in a short QPC when only $\lambda_F^{\uparrow}$ is big enough to render a bound state. The remaining up-spin conduction channel then gives rise to a $0.5G_0$ plateau.[10]

Semiclassically we can use the Hamiltonian equations of motion, $\partial H_x^{\text{eff}}/\partial x = -\dot{P}_x$ and $\partial H_x^{\text{eff}}/\partial P_x = \dot{x}$, to derive an effective potential,

$$V_x^{\text{eff}} = \left(n + \frac{1}{2}\right)\hbar\varpi_y(x) - m_{\text{eff}}\alpha^2 E_z^2(x) = V_{\text{conf}}(x) + V_{\text{Rashba}}(x), \tag{6}$$

which consists of two competing terms (see Fig. 1). The confining potential in the y direction tends to push the electrons out of the QPC, while the RI favors trapping them inside. Whether a deep well can be formed depends on the strength and nonuniformity of E_z.

Now we need to calculate how E_z varies in the x direction due to V_g. The front edges of the side gates function as a capacitance because the 2DEG is grounded and V_g is applied on the tips above. So the E_z from these capacitance wires can be calculated as $w\rho/2\pi\epsilon\int_{-L/2}^{L/2} dx/[(x-x_0)^2+y_0^2]^{3/2}$, where w is the thickness of 2DEG, $\rho = Q/(L+\sqrt{A}) \sim 2\sqrt{A\epsilon V_g}/w$, A is the area of the gate, ϵ represents the dielectric constant, and y_0 and L are the width and length of the QPC. After the integration, E_z is obtained as

$$E_z(x) = \frac{\sqrt{A}}{\pi y_0^2} V_g \left[\frac{\frac{L}{2} - x}{\sqrt{\left(\frac{L}{2} - x\right)^2 + y_0^2}} + \frac{\frac{L}{2} + x}{\sqrt{\left(\frac{L}{2} + x\right)^2 + y_0^2}} \right]. \tag{7}$$

As we can see, high gate voltage, small QPC width, and large QPC length all enhance the nonuniformity of E_z, which is stronger in the middle of the QPC—the same trend as the strength of RI.

Let us compare the magnitude of the two terms in Eq. (6). First, we figure out the exact Rashba coefficient near the QPC by measuring the magnetoresistance.[9] Then, by tuning V_g we can control the strength of RI. The order of $\hbar\varpi_y$ can be estimated by counting the number N of plateaus below some specific gate voltage, which tells us that $\epsilon_F \geq (N+0.5)\hbar\varpi_y$ and $\hbar\varpi_y(V_g) \sim 1$ meV. On the other hand, the order of RI is about 10^{-12} eV m (Refs. 12 and 13) and $\lambda_F \sim 10^8$ m^{-1}. So the Rashba energy is of the order of 0.1 meV. In particular, the E_z within a QPC tips should be much stronger due to their sharp geometry so that the orders of these two terms in Eq. (6) are expected to be comparable. Finally, we plug Eq. (7) into Eq. (6). The resultant $V_x^{\text{eff}}(x, L, V_g)$ is plotted in Fig. 2 for a medium-size QPC ($L=200$ nm), from which we can see the qualitative profile of the potential and how it evolves with V_g.

When V_g is weak, both $n=0,1$ surfaces in Fig. 2 exhibit a saddlelike profile with no bound state, consistent with the experimental observation.[14] As V_g gets stronger, a potential well starts to appear in the middle of the QPC which can sustain bound states. This provides the direct evidence for the feasibility of the Kondo model to explain the 0.7 anomaly.[2] The characteristic energy scale of the Kondo model is the Kondo temperature[15] $T_K \sim \Delta E \times \exp\{-[(e^2/h)/G]E_C/\Delta E\}$, where $\Delta E \sim \hbar^2/(m_{\text{eff}}R^2)$ denotes the level spacing, R and E_C represent the linear size and

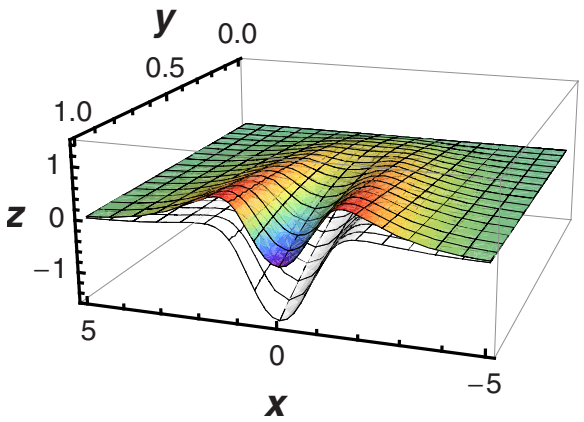

FIG. 2. (Color online) Effective potential under the semiclassical approximation for a medium QPC of length $L=200$ nm. The x axis represents the spatial coordinate along the QPC, while the y axis denotes V_g and the z axis is the effective potential. The upper/lower surfaces represent the $n=1/0$ channels. The higher the V_g, the deeper the well. This potential well and its ability to trap electrons are essential to the Kondo model for the 0.7 anomaly.

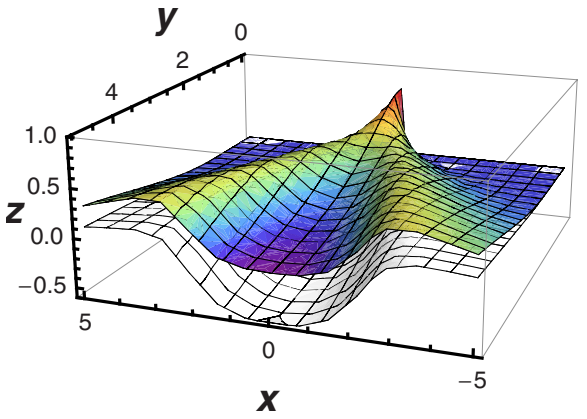

FIG. 3. (Color online) The y axis denotes the length of the QPC, while the notations for x and z axes are the same as in Fig. 2. The V_g is set at 0.5 V. The top/bottom surfaces represent $n=1/0$ channels, respectively. A short QPC does not favor the formation of bound state. On the other hand, higher channels for a long QPC may exhibit bound states, which we propose to be responsible for the 1.7 shoulder.

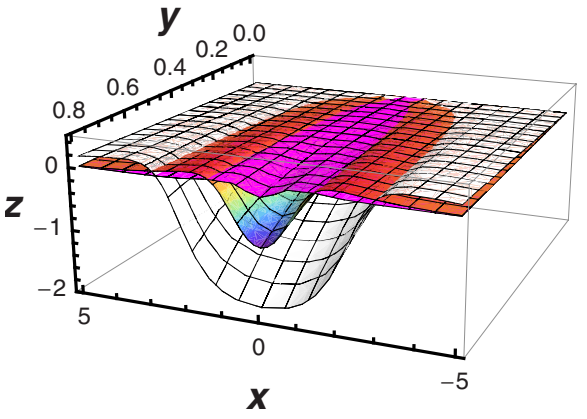

FIG. 4. (Color online) From top to bottom, the potential is plotted for short, medium, and long QPCs, respectively, as a function of gate voltage in the y axis. The notations for x and z axes are the same as in Fig. 2. In the top surface there is no bound state. The potential profile in the middle surface resembles that of a small QD, for which the 0.7 plateau arises from the Kondo effect. Finally, the lowest surface for the long QPC is equivalent to a big QD where an interesting dip shows up at $0.5G_0$ due to the CB.

charging energy of the QD, and $E_C/\Delta E$ roughly equals to the ratio of R and the effective Bohr radius. The conductance of the dot-lead junction $G=G_L+G_R$ consists of the left- and right-going parts, which can be derived from the Landauer formula[16] $G_L=G_R=(2e^2/h)\Sigma t_n^* t_n$, where t_n is the transmission coefficient of the nth conducting channel. By the WKB approximation,[17] $t_0=4/(2\theta+1/2\theta)^2$, where $\theta=\exp\{\int dx\sqrt{2m_{\rm eff}[V_{\rm eff}^{(n=0)}(x)-E_F]}/\hbar\}$ and $V_{\rm eff}^{(n=0)}(x)$ is the $n=0$ potential profile in Fig. 2. We estimate T_K to be of the order of a few hundred millikelvins, and it decreases as the gate voltage increases. These are in line with the experimental observation.[3]

We may now proceed to discuss how the length of the QPC affects the bound-state formation. Figure 3 shows $V_x^{\rm eff}(x,L,V_g)$ for fixed $V_g=0.5$ V. If QPC is too short and λ_F is too small, there is no potential well. As QPC increases in size or for a larger λ_F, a potential well emerges and becomes deeper and broader. Bound states can occur in high channels ($n\geq 1$) for the long QPC, as can be seen in Fig. 3. We believe this is responsible for the rare 1.7 or $2.7G_0$ shoulder that appeared in some experiment.[10] They are more difficult to form than in the $n=0$ channel.

We can compare Fig. 4 qualitatively with the experiments[10] which reported the evolution of plateaus. The bottom surface is for a long QPC ($L=500$ nm) which corresponds to Fig. 3 of Ref. 10, while the middle one for a medium QPC ($L=200$ nm) is contrasted with Fig. 2 of Ref. 10. The top surface is for a short QPC ($L=100$ nm). The deciding parameter γ measures how dramatic the electric field varies within a QPC. $\gamma\gg 1$ in the first two cases compares to $\gamma\ll 1$ in the last case. In Fig. 2 of Ref. 10, the $0.7G_0$ (the rightmost) evolves continuously to $0.55G_0$ (the leftmost) with increasing electron density or k_F. This has the same effect on γ as shortening the QPC, as exemplified by the transition from the middle to the top surfaces in Fig. 4. According to the top surface in Fig. 4, there is no bound state at small V_g. However, if the $\lambda_F^{\uparrow}$ is large enough to make γ sizable, its bound state might render the up-spin conduction channel ineffective. This corresponds to the leftmost line in Fig. 2 of Ref. 10 that indeed only shows a plain plateau around $0.5G_0$. The middle surface in Fig. 4 corresponds to the rightmost line in Fig. 2 of Ref. 10 for a dilute carrier density because both satisfy $\gamma\gg 1$. Note that it may look confusing why the short QPC in Fig. 1 of Ref. 10 gives rise to $0.7G_0$ instead of 0.5. The reason is that its λ_F is relatively large which compensates the shortness of L and still renders $\gamma\gg 1$. We believe the 0.5 plateau will emerge if they[10] further decrease λ_F.

In Fig. 3 of Ref. 10, a long QPC was used and a dip instead of a shoulder showed up near $0.5G_0$. We believe this corresponds to the bottom surface in Fig. 4. The bound electron is localized in a larger region than that of the middle surface. This resembles the confinement of a big QD (Ref. 8) where the dip can be linked[18] to the characteristic behavior of the CB. This is in contrast to the narrow confinement in the middle surface of Fig. 4, mimicking a small QD, which provides a localized moment for the Kondo resonance and leads to the 0.7 structure and ZBA.

Let us now turn to the recent experiment by Sfigakis *et al.*[18] who suggested that a weakly bound state might have been formed in a clean QPC because it shared many characteristics with their open quantum dots. We agree with their interpretation for the dip feature when $\Delta V_g=0$ due to the CB from the wide confinement resembling a big QD. However, the fact that the first dip occurs around $0.5G_0$ and the 1.7 structure, as in the case of long QPC,[10] is more naturally explained by our picture. Namely, the former comes from the CB, while the latter arises from the Kondo resonance with the bound state in $n=1$ channel. Sfigakis *et al.*[18] found two temperature (T) dependences for the dip around $0.5G_0$: (1) it disappeared while the conductance increases as they lowered T and (2) it evolved into a 0.7 shoulder when T was increased. They thus concluded that the quantum dot Kondo

model, which fit their low-T data, played no part in the making of the 0.7 shoulder at high T. After a closer look at their data, we found that a 0.7 shoulder at low T in their Fig. 2(b) could not be excluded, which was more outstanding in our view than the 0.7 shoulder they claimed to see at high T in their Fig. 2(c) —possibly misled by the crossing of different-temperature lines. We can also explain another feature in the data of Sfigakis *et al.*[18] which they did not emphasize, which is the evolution of the 1.7 shoulder to the $2G_0$ plateau in their Fig. 2(a) as T is lowered. In our theory, the 1.7 shoulder is not different from the 0.7 anomaly such that both are caused by the bound state and its resulting Kondo resonance. So its evolution with T can be understood in the same way as the similar evolution of the 0.7 shoulder to $1G_0$ in their Fig. 1(a) for $\Delta V_g \neq 0$ and another experiment on QPC.[3] The explanation based on the Kondo model can be found in Ref. 2. In the geometric structure Sfigakis *et al.*[18] designed, the conductance of the dot-lead junction G is suppressed as V_g increases, which leads to a lower T_K. This is consistent with their observation[18] that the $1.7G_0$ shoulder evolved into a dip at $0.5G_0$ as V_g increased. The former was kept alive by the high T_K at low V_g, while the CB replaces and dominates the Kondo physics at high V_g.

In conclusion, we propose that a bound state can be formed within a QPC if RI is taken into account with a nonuniform E_z produced by the side gates. Such a bound state provides evidence to the feasibility of the Kondo scenario to explain the 0.7 structure. Whether bound states can exist relies partially on the degree of nonuniformity of E_z which depends sensitively on the gate voltage, QPC length, and the Fermi wavelength. A semiclassical approximation is used to help us visualize the bound states as a function of V_g and L. We are able to provide a coherent theory that covers three main features: a 0.5 plateau, a 0.7 structure, and a dip at $0.5G_0$. The origin of the rare $1.7G_0$ plateau is also discussed, and the temperature dependence of each feature is well accounted for. According to our survey, the 0.7 anomaly indeed was more distinct in p-type GaAs (Ref. 19) and $In_{1-x}Ga_xAs$ (Ref. 20) than in Si/SiGe.[21] However, cautions are required when making such a comparison since a high mobility and large γ are also indispensable.

We benefited from discussions and correspondence with Jen-Chung Chen, Chi-Te Liang, Hsiu-Hau Lin, and Yigal Meir. Support by NSC in Taiwan under Grant No. 95-2120-M007-008 is acknowledged.

[1] A very recent survey and discussions on this topic can be found in J. Phys.: Condens. Matter **20**, No. 16 (2008).
[2] Yigal Meir, Kenji Hirose, and Ned S. Wingreen, Phys. Rev. Lett. **89**, 196802 (2002); T. Rejec and Y. Meir, Nature (London) **442**, 900 (2006).
[3] S. M. Cronenwett, H. J. Lynch, D. Goldhaber-Gordon, L. P. Kouwenhoven, C. M. Marcus, K. Hirose, N. S. Wingreen, and V. Umansky, Phys. Rev. Lett. **88**, 226805 (2002).
[4] K. J. Thomas, J. T. Nicholls, M. Y. Simmons, M. Pepper, D. R. Mace, and D. A. Ritchie, Phys. Rev. Lett. **77**, 135 (1996).
[5] A. C. Graham, K. J. Thomas, M. Pepper, M. Y. Simmons, and D. A. Ritchie, Physica E **22**, 264 (2004).
[6] Chi-Te Liang (private communication).
[7] David Sanchez and Llorenc Serra, Phys. Rev. B **74**, 153313 (2006).
[8] Henrik Bruus and Karsten Flensberg, *Many-Body Quantum Theory in Condensed Matter Physics* (OUP, Oxford, 2004).
[9] J. Nitta, T. Akazaki, H. Takayanagi, and T. Enoki, Phys. Rev. Lett. **78**, 1335 (1997).
[10] D. J. Reilly, G. R. Facer, A. S. Dzurak, B. E. Kane, R. G. Clark, P. J. Stiles, J. L. O'Brien, N. E. Lumpkin, L. N. Pfeiffer, and K. W. West, Phys. Rev. B **63**, 121311(R) (2001).
[11] B. J. van Wees, H. van Houten, C. W. J. Beenakker, J. G. Williamson, L. P. Kouwenhoven, D. van der Marel, and C. T. Foxon, Phys. Rev. Lett. **60**, 848 (1988).
[12] Ehud Shafir, Min Shen, and Semion Saikin, Phys. Rev. B **70**, 241302(R) (2004).
[13] J. B. Miller, D. M. Zumbühl, C. M. Marcus, Y. B. Lyanda-Geller, D. Goldhaber-Gordon, K. Campman, and A. C. Gossard, Phys. Rev. Lett. **90**, 076807 (2003).
[14] Y. Yoon, L. Mourokh, T. Morimoto, N. Aoki, Y. Ochiai, J. L. Reno, and J. P. Bird, Phys. Rev. Lett. **99**, 136805 (2007).
[15] Michael Pustilnik and Leonid Glazman, J. Phys.: Condens. Matter **16**, R513 (2004).
[16] R. Landauer, IBM J. Res. Dev. **1**, 233 (1957); Philos. Mag. **21**, 863 (1970).
[17] E. Merzbacher, *Quantum Mechanics* (Wiley, New York, 1998).
[18] F. Sfigakis, C. J. B. Ford, M. Pepper, M. Kataoka, D. A. Ritchie, and M. Y. Simmons, Phys. Rev. Lett. **100**, 026807 (2008).
[19] L. P. Rokhinson, L. N. Pfeiffer, and K. W. West, Phys. Rev. Lett. **96**, 156602 (2006); A. R. Hamilton, R. Danneau, O. Klochan, W. R. Clarke, A. P. Micolich, L. H. Ho, M. Y. Simmons, D. A. Ritchie, M. Pepper, K. Muraki, and Y. Hirayama, J. Phys.: Condens. Matter **20**, 164205 (2008).
[20] P. J. Simmonds, F. Sfigakis, H. E. Beere, D. A. Ritchie, M. Pepper, D. Anderson, and G. A. C. Jones, Appl. Phys. Lett. **92**, 152108 (2008).
[21] G. Scappucci, L. Di Gaspare, E. Giovine, A. Notargiacomo, R. Leoni, and F. Evangelisti, Phys. Rev. B **74**, 035321 (2006).